Proliferative and Transcriptional Identity of Distinct Classes of Neural Precursors in the Mammalian Olfactory Epithelium

Proliferative and transcriptional identity of distinct classes of neural precursors in the mammalian olfactory epithelium

Eric S. Tucker[1]*, Maria K. Lehtinen[2], Tom Maynard[1†,] Mariela Zirlinger[3], Catherine Dulac[3], Nancy Rawson[4], Larysa Pevny[5,6] and Anthony-Samuel LaMantia[1,6,†‡]

[1] Department of Cell and Molecular Physiology, University of North Carolina at Chapel Hill, NC 27599, USA.

[2] Howard Hughes Medical Institute, Division of Genetics, Children's Hospital Boston, Chevy Chase, MD 20815-6789, USA.

[3] Department of Molecular and Cellular Biology, Harvard University, Cambridge MA, 02138, USA.

[4] Monell Chemical Senses Center, Philadelphia, P19104, USA.

[5] Department of Genetics, University of North Carolina at Chapel Hill, NC 27599, USA.

[6] UNC Neuroscience Center, University of North Carolina at Chapel Hill, NC 27599, USA.

* Present address: Centre for Neuroscience, West Virginia University School of Medicine, Morgantown, WV 26506, USA.

† Present address: George Washington Institute for Neuroscience, George Washington University School of Medicine, Washington, DC 20037, USA.

‡ Author for correspondence (phmasl@gwumc.edu)

Summary

Neural precursors in the developing olfactory epithelium (OE) give rise to three major neuronal classes – olfactory receptor (ORNs), vomeronasal (VRNs) and gonadotropin releasing hormone (GnRH) neurons. Nevertheless, the molecular and proliferative identities of these precursors are largely unknown. We characterized two precursor classes in the olfactory epithelium (OE) shortly after it becomes a distinct tissue at midgestation in the mouse: slowly dividing self-renewing precursors that express Meis1/2 at high levels, and rapidly dividing neurogenic precursors that express high levels of Sox2 and Ascl1. Precursors expressing high levels of Meis genes primarily reside in the lateral OE, whereas precursors expressing high levels of Sox2 and Ascl1 primarily reside in the medial OE. Fgf8 maintains these expression signatures and proliferative identities. Using electroporation in the wild-type embryonic OE in vitro as well as *Fgf8, Sox2* and *Ascl1* mutant mice in vivo, we found that Sox2 dose and Meis1 – independent of Pbx co-factors – regulate Ascl1 expression and the transition from lateral to medial precursor state. Thus, we have identified proliferative characteristics and a dose-dependent transcriptional network that define distinct OE precursors: medial precursors that are most probably transit amplifying neurogenic progenitors for ORNs, VRNs and GnRH neurons, and lateral precursors that include multi-potent self-renewing OE neural stem cells.

INTRODUCTION

The olfactory epithelium (OE) differentiates from the lateral surface ectoderm of the vertebrate head, and gives rise to three major neuron classes: olfactory receptor neurons (ORNs), vomeronasal receptor neurons (VRNs) and gonadotropin releasing hormone (GnRH) neurons. ORNs and VRNs detect and relay information about a vast range of chemicals essential for feeding, reproduction and social interactions (for reviews, see Ache and Young, 2005; Buck, 2000; Dulac and Torello, 2003). GnRH neurons migrate from the OE to the hypothalamus (Schwanzel-Fukuda and Pfaff, 1989; Wray et al., 1989), where they regulate reproduction (Foster et al., 2006). Despite the functional importance of ORNs, VRNs and GnRH neurons, the identity of OE precursors remains uncertain. Furthermore, it is not know how local inductive signals or transcription factors distinguish proliferative and neurogenic capacities. Solving these longstanding mysteries not only provides insight into developmental specification of these essential yet inadequately characterized precursors, it addresses a central issue in regeneration: embryonic OE precursors must give rise to adult counterparts that generate ORNs and VRNs throughout life (reviewed by Schwob, 2002). Thus, we determined cellular and molecular mechanisms that define identity, proliferation and neurogenic potential of the earliest OE neural precursors.

OE neuronal precursors, such as those in other nervous system regions (for reviews, see Gotz and Huttner, 2005; Jessell and Sanes, 2000; Livesey and Cepko, 2001), should be found in discrete locations, have characteristic gene expression, distinct proliferative kinetics and the unique capacity to generate all differentiated OE neuron classes. Cells expressing neurogenic bHLH transcription factors, particularly Ascl1, have been proposed as OE precursors (Beites et

al., 2005; Cau et al., 1997); however, persistence of ORNs despite loss of Ascl1 function (Guillemot et al., 1993) indicates that other precursors can generate OE neurons. Accordingly, we determined relationships between additional transcription factors, and cells with distinct proliferative or differentiation capacity among the earliest OE precursors. We found substantial differences in OE precursor identity at midgestation: slowly dividing, self-renewing precursors expressing high levels of Meis genes populate primarily the lateral OE, whereas rapidly dividing neurogenic precursors expressing high levels of *Sox2* and *Ascl1* reside mostly in the medial OE. These identities are established in part by Fgf8, and a transcriptional network involving Sox2 dose, Meis1 activity and Ascl1 expression that regulates progression from multipotent precursor to transit amplifying neuronal progenitor to post-mitotic neuron. Our findings suggest that among primarily lateral, Meis-expressing OE precursors are stem cells whose presence guarantees initial genesis of ORNs, VRNs and GnRH neurons.

MATERIALS AND METHODS

Animals

Mouse embryos were harvested from timed-pregnant mothers (plug day=0.5) maintained by the Department of Laboratory Animal Medicine at the University of North Carolina at Chapel Hill or Children's Hospital (Boston, MA, USA). The *Sox2* indicator (Ellis et al., 2004) was bred into CF-1 females from $Sox2^{eGFP/+}$ males. $Fgf8^{neo/neo}$ (Meyers et al., 1998) and $Ascl1^{-/-}$ embryos (Guillemot et al., 1993) were generated from $Fgf8^{neo/+}$ or $Ascl1^{+/-}$ males and females, respectively. $Sox2^{hyp/-}$ embryos were generated from $Sox2^{eGFP/+}$ males and $Sox2^{hyp/+}$ females

(Taranova et al., 2006). Dams were killed by rapid cervical dislocation, and embryos were collected and genotyped using appropriate PCR primers. Institutional Animal Care and Use Committees (IACUC) at UNC-CH and CHB approved all procedures.

Immunohistochemistry

Embryos were fixed with 4% paraformaldehyde, embedded and cryosectioned using standard methods. Primary antibodies were obtained commercially [NCAM (Chemicon/Millipore), PH3 (Chemicon/Millipore), TuJ1 (Babco), OMP (Wako), Pbx1/2/3, ACIIII (Santa Cruz), BrdU (Becton-Dickinson), IdU (Accurate Chemical and Scientific) and Ascl1 (Becton-Dickinson)] or as gifts [Meis1 and Meis2 (A. Buchberg, Thomas Jefferson University), and GnRH (S. Wray, NINDS)]. The Sox2 antiserum was produced by L. Pevny's laboratory, and TrpC2 antiserum by C. Dulac's laboratory. Images were obtained using a Leica DMR epifluorescence or Zeiss LSM510 laser-scanning confocal microscope.

Cell cycle measurement

We estimated cell cycle times using dual DNA synthesis labeling (Martynoga et al., 2005). Iodinated deoxyuridine (IdU) was injected initially (T0), intraperitoneally (i.p.; 70 mg/kg body weight) in pregnant dams followed by bromodeoxyuridine (BrdU; 50 mg/kg) 1.5 hours later (T1). After an additional 0.5 hours (T2), embryos are fixed for IdU/BrdU histochemistry. The mouse anti-BrdU antibody BrdU detects both IdU and BrdU; however, the rat anti-BrdU antibody is specific. Thus, cells remaining in S-phase during the 2-hour period are double-labeled; IdU-labeled cells exit the cell cycle. S-phase (TS) and total cell cycle length (TC) is calculated as: TS=1.5/(number IdU labeled/number double-labeled cells), TC=TS/(number

double-labeled/number all cells – identified by nuclear staining). We divided each OE section into ten sectors representing equivalent parts of its total length, and calculated TS and TC for each sector in a full series (7-10 sections) from five E11.5 embryos. Statistical analysis was performed using analysis of variance (ANOVA) followed by Tukey's honestly significant difference test.

Short- and long-term BrdU labeling

BrdU was injected i.p. at E9, E10 or E11, followed by 2-hour (DNA synthesis) or 5.5- to 6.5-day (birthdating) survival. For label retention, we adapted a long-term BrdU labeling protocol (Morshead et al., 1994); BrdU (50 mg/kg) was injected i.p. in pregnant dams at E9, with a second injection 4 hours later. Upon first injection, we provided 1 mg/ml BrdU as drinking water, and left this in place until E11.5. Thereafter, pregnancy continued, with no further BrdU exposure, until E16.5 when fetuses were collected for BrdU histochemistry.

Pair cell assays

The lateral and medial OE was microdissected from entire E11.5 litters (n=4 independent experiments/4 litters), and dissociated as described (Shen et al., 2002). Dissociated cells were plated at clonal density on poly-D lysine coated Terasaki plates. Some cell suspensions received Fgf8 (100 nM) prior to plating. Cultures were fixed after 20 hours, co-labeled for TuJ1 with Meis1 or Sox2, as well as bisbenzimide to identify nuclei. `Paired' bisbenzimide-labeled nuclei were identified in individual wells, and expression of neuronal and transcription factor markers was visualized and scored.

Explant electroporation, staining and analysis

E11.5 lateral nasal processes (LNPs) were micro-dissected, and up to six LNPs at a time were transferred to an electroporation chamber (Protech International, San Antonio, TX) with 50 µl of 3 mg/ml endotoxin-free control or Sox2, Meis1 or Meis1/Pbx1 DNA plasmids (Sigma) in HBSS (Invitrogen). LNP luminal (OE) surfaces were electroporated with five 50 ms pulses at 30 V separated by a 950 ms inter-pulse delay using an ECM 830 electroporator (BTX). LNPs were transferred to membrane filters (luminal surface up), grown 72 hours in vitro, fixed and immunostained (Tucker et al., 2006). Images of five non-overlapping fields were collected at 63× from each explant with a Zeiss510 laser-scanning confocal microscope. Double-labeled cell frequencies were compared between conditions by a two-tailed unpaired Student's *t*-test.

RESULTS

Medial and lateral OE precursors are molecularly distinct

At E11.5, shortly after the OE invaginates, graded expression of several transcription factors defines OE domains. Sox2, an essential SoxB1 factor in the OE (Donner et al., 2007), recognized with an antibody (Fig. 1A) or Sox2-eGFP indicator transgene (Fig. 1E) (Ellis et al., 2004) is expressed at low levels in the ventrolateral OE and progressively higher levels in the dorsomedial OE. The proneural basic helix-loop-helix transcription factor Ascl1 (formerly Mash1) is also expressed in a subset of dorsomedial OE cells where Sox2 levels are higher (Fig. 1B). Conversely, Meis1 (Toresson et al., 2000) (Fig. 1C), Meis2 (not shown) and Pbx1/2/3 (Fig. 1D) are concentrated primarily in the lateral OE (see also Fig. 2). Graded expression patterns of

Sox2, Meis1 and Ascl1 appear related: Sox2 expression is typically lowest where Meis1 is highest (Fig. 1E). Ascl1 is seen in regions where Meis1 expression is diminished, and Sox2 expression enhanced (Fig. 1F). Finally, in the ventromedial OE, both Meis1 and Sox2 levels are elevated, and Ascl1 and Pbx are not seen (Fig. 1A-D). Thus, graded transcription factor expression defines a primarily lateral OE domain where Meis1 is elevated, Sox2 and Pbx1 expression varies, and Ascl1 is absent, a primarily medial domain where Ascl1 and Sox2 are elevated, Meis1 varies and Pbx1 is absent, and a ventro-medial domain where both Meis1 and Sox2 are elevated, and Ascl1 is not seen.

Neuronal markers identify cells with morphological and molecular characteristics of ORNs, VRNs and GnRH neurons in the nascent OE (Fig. 1G-K). Presumptive ORNs and VRNs, labeled with neuronal markers such as class III β-tubulin (TuJ1) (Fig. 1G,H) and NCAM (data not shown) have characteristic bipolar morphologies, including an immature apical dendritic knob and a single axon that extends from the OE through the mesenchyme (Fig. 1H and inset). VRNs are distinguished by co-expression of the TrpC2 channel, which is functionally associated with this subclass of chemosensory neurons (Stowers et al., 2002) primarily in the presumptive vomeronasal organ (pVNO) (Fig. 1I and inset). Finally, GnRH neurons are found in the pVNO epithelium (Fig. 1J) and in the adjacent mesenchyme (Fig. 1K), migrating toward the basal forebrain. Neuronal labeling begins in the dorsolateral OE (Fig. 1G), where Sox2/Ascl1 levels increase and Meis/Pbx levels decline (Fig. 1E,F, sector c), and ends in the ventromedial OE, where Sox2 is elevated (Fig. 1A, left of asterisk), Ascl1 is absent and Meis levels rise. Therefore, at E11.5, three major classes of neurons are concentrated around the medial OE, with presumed ORNs in dorsolateral through dorsomedial regions, VRNs most frequent in medial to ventromedial domains and GnRH neurons primarily in the ventromedial OE.

Distinct modes of cell proliferation in lateral and medial OE precursors

We next asked whether molecularly defined OE domains include precursors with distinct proliferative capacities. At E11.5, M-phase cells, recognized by phospho-histone 3 (PH3), are most frequent in the medial OE (Fig. 2A,B). PH3-labeled nuclei appear concentrated at the apical surface, with no apparent mediolateral differences in apical/basal distribution. Cells in the lateral OE are more likely to be in S-phase, based upon frequency of acutely BrdU-labeled cells (Fig. 2C,D). Most S-phase cells in the lateral OE also express Meis1 at high levels; however, few of the scattered medial OE cells that express low levels of Meis1 co-label with BrdU (Fig. 2C,D; see also Fig. 1C). The inverse relationship between S- and M-phase precursors suggests that cell cycle lengths may differ in register with molecular distinctions (Fig. 2E,F). Precursors in the ventromedial OE (particularly sector 1, Fig. 2E) that express Meis1, as well as high levels of Sox2 (Fig. 1A,C), have longer cell cycles and lower mitotic frequency, as do other Meis1-expressing lateral precursors (especially including sectors 2-4) in which Sox2 levels decline and Pbx is seen (Fig. 2F). In precursors in the remaining OE sectors, where Sox2 expression is more robust, Ascl1 is seen, the neurons are concentrated and have shorter cell cycle times. Apparently, Meis1 levels may have a more substantial influence on cell cycle length than Sox2, Pbx or Ascl1 levels.

S-phase appears constant across the OE (Fig. 2E,F), suggesting longer cell cycles in ventral and lateral OE precursors reflect longer G1-S transitions. Therefore, we asked whether lateral OE cells are more likely to retain BrdU for long periods, a signal that is characteristic of slowly dividing, multipotent neural stem cells (Morshead et al., 1994). Following chronic BrdU exposure (E9-E11.5) and additional 5-day survival (E16.5), a significant proportion of Meis1-

labeled (Fig. 2G,I-K) as well as Sox2-labeled (Fig. 2H,L-N) basal cells in the lateral OE are also heavily labeled with BrdU (29% Meis1 cells/87 total cells counted; 22% Sox2 cells/18 total cells counted; *n*=4 animals). We found no medial Sox2 or Ascl1 cells heavily BrdU-labeled (Fig. 2O,P); however, a small number were faintly labeled (Fig. 2O, inset; 4% Sox2 cells/104 total cells counted; 2% of Ascl1 cells/83 total cells counted; *n*=4 animals). By contrast, a significant proportion of OMP-labeled ORNs in the medial OE are heavily BrdU labeled (54% OMP cells/31 total cells counted; *n*=4 animals). Thus, based upon frequency, kinetics and distribution of M- and S-phase markers, lateral and medial OE domains contain two distinct proliferative populations – one slowly dividing and another rapidly dividing – in register with differing levels of Meis1.

Meis1-positive OE precursors, concentrated in the lateral OE, may divide slowly and symmetrically to maintain multipotent precursors while the remaining precursors, primarily those in the medial OE, divide rapidly and terminally to expand the neuronal population. Accordingly, we determined the mode and consequences of single cell divisions from E11.5 micro-dissected lateral and medial OE using a pair cell assay (Shen et al., 2002). Pairs (two progeny from single OE cells after 20 hours in vitro) were classified as neuron-neuron (N-N; Fig. 3A, top), neuron-precursor (N-P; Fig. 3A, bottom) or precursor-precursor (P-P; Fig. 3B,C) based upon co-labeling for TuJ1, Sox2 and bisbenzamide or for TuJ1, Meis1 and bisbenzamide. TuJ1-positive cells were counted as neurons; Sox2- or Meis1-positive/TuJ1-negative cells were counted as precursors. Pairs stained with bisbenzimide only – unrecognized OE precursors, particularly those for non-neuronal or vascular cells, or mesenchymal cells that remain after incomplete removal of OE-adherent mesenchyme – were designated as precursor*-precursor* (P^{*}-P^{*}; Fig. 3D) and counted separately. The absence of Sox2 labeling in these P^{*}-P^{*} pairs

suggests they are unlikely to be OE neural precursors. Meis1 (Fig. 3B) and Sox2 (Fig. 3C, top) pairs were found at similar frequencies in lateral OE cultures, and combined in P-P totals; medial cells, however, preferentially generated Sox2 pairs (Fig. 3C, bottom) and rarely labeled for Meis1. The primary mode of cell division for isolated lateral and medial OE precursors was symmetric (Fig. 3E). Lateral cells, however, generated significantly more P-P pairs (51.1±3.6% of 327 total lateral versus 7.6±0.4% of 251 total medial pairs from three independent experiments; $P \leq 0.006$, Mann-Whitney) and medial cells significantly more N-N pairs (49±2.1% medial versus 16.8±2.9% lateral, $P \leq 0.006$). Each region generated small percentages of N-P pairs (4.4±0.4% medial versus 2.8±0.7% lateral; no difference). Thus, lateral OE precursors are primarily self-renewing, producing additional precursors, and medial OE precursors are primarily neurogenic.

Fgf8 promotes OE neurogenesis by repressing Meis1 and enhancing Sox2

Self-renewal versus terminal neurogenesis may be regulated by exposure to inductive signals that influence initial OE differentiation in vitro or in vivo (Kawauchi et al., 2005; LaMantia et al., 2000). Based on previous observations that Fgf8 enhances neurogenesis in the OE (DeHamer et al., 1994; Kawauchi et al., 2005; LaMantia et al., 2000), we asked whether Fgf8 increases symmetric neurogenic divisions in lateral OE cells at the expense of divisions favoring self-renewal. When lateral OE precursors are treated with Fgf8, the frequency of N-N pairs increases twofold (Fig. 3E, bottom; 34±3.2% of 386 total pairs, three independent experiments versus 16.8±2.9% lateral control, 51% increase, $P \leq 0.01$) and P-P pairs decline similarly (28.1±4.9 Fgf8 versus 51.1±3.5% lateral control, 46% decline, $P \leq 0.01$). P^*-P^* pairs also increased in response to Fgf8 (42.9% of Fgf8 versus 29.4%, lateral control, 32% increase $P \leq 0.045$); however, this may

reflect general mitogenic activity of Fgf8. Nevertheless, Fgf8 apparently enhances neurogenesis in lateral OE precursors from by promoting symmetrical, terminal, neurogenic divisions and diminishing self-renewal of precursors that express Meis1 or Sox2.

Based on these in vitro findings, we hypothesized that Fgf8, which is available from the medial OE in vivo (Bhasin et al., 2003; Kawauchi et al., 2005; LaMantia et al., 2000), establishes or maintains OE precursor distinctions. To test this genetically, we evaluated OE precursors in E11.5 hypomorphic embryos, in which Fgf8 levels are significantly reduced but not eliminated (*Fgf8*$^{neo/neo}$) (Meyers et al., 1998). *Fgf8*$^{neo/neo}$ embryos display variably penetrant phenotypes as previously reported (Garel et al., 2003; Meyers et al., 1998). Three out of 6 *Fgf8*$^{neo/neo}$ embryos had forebrain morphogenetic defects, including rostromedial extension of ventral telencephalic neuroepithelium (see Fig. S1 in the supplementary material) and no morphologically identifiable VNO; the remainder displayed relatively normal morphologies. Altered OE transcription factor expression was apparent in five embryos, most noticeably in those with forebrain dysmorphology (Fig. 3 and see Fig. S1 in the supplementary material). Sox2 is diminished in the medial OE of *Fgf8*$^{neo/neo}$ embryos (Fig. 3F), and the wild-type gradient is difficult to discern (compare with Fig. 1A,E). Meis1 shifts medially (Fig. 3G,J; see Fig. S1D,F,I in the supplementary material) but declines dorsolaterally (Fig. 3G,J) where neurons are found (Fig. 3H). Neurogenesis, though attenuated, extends into regions where Meis1 is elevated (Fig. 3G,H). Ascl1 expression varies in *Fgf8*$^{neo/neo}$ embryos (highest frequency, Fig. 3I,J; lowest frequency, see Fig. S1L in the supplementary material); however, remaining Ascl1 precursors appear diminished medially and shifted laterally (Fig. 3I; see Fig. S1F,L in the supplementary material). Apparently, Fgf8 promotes OE neurogenesis by enhancing Sox2 and Ascl1 expression, and restricting Meis1 expression.

A Sox2-dependent transcriptional network defines OE precursor identity

OE precursors are distinguished by position-dependent expression of Sox2, Meis, Ascl1 and Pbx, suggesting that these transcription factors may be key regulators of their identity. Thus, we developed an in vitro E11.5 lateral OE preparation to ectopically express these factors and evaluate directly their influence on identity and neurogenic capacity (Fig. 4A). We first asked whether Sox2 dose regulates lateral versus medial precursor distinctions by electroporating a chicken β-actin/cytomegalovirus promoter that drives mouse *Sox2* followed by an internal ribosome entry site (IRES) and *eGFP* (pCIG-Sox2; Fig. 4B,C). For quantification, five non-overlapping fields were sampled ventral to the transition zone where Sox2 and Ascl1/TuJ1 levels rise and Meis1 levels decline (Fig. 4A). Elevated Sox2 dose elicits three cell-autonomous changes within the ventrolateral OE. First, ectopic overexpression of Sox2 diminishes the frequency of Meis1-expressing cells (93±0.48%/100 control-electroporated cells versus 10±0.87%/100 Sox2-electroporated cells, $P<0.00001$; Fig. 4D-H). Second, overexpression of Sox2 increases the frequency of Ascl1 cells (3.1±1.18%/2217 control versus 33.1±3.06%/1585 Sox2-electroporated cells, $P<0.00002$; Fig. 4I-M). Third, raising Sox2 levels enhances the number of TuJ1-labeled OE neurons (1.1±0.86%/2021 control cells versus 13.2±1.27%/1161 Sox2-electroporated cells, $P=0.0002$; Fig. 4N-T). Thus, ectopic Sox2 overexpression imposes a more `medial' character on lateral OE precursors: Meis1 levels are reduced, Ascl1 expression is elevated and neurogenesis is enhanced.

We next asked whether Meis or Pbx regulates acquisition or retention of `lateral' OE characteristics. We over-expressed Meis1 alone (pCIG-Meis1) or in combination with Pbx1 (pCIG-Meis1-IRES-Pbx1) using a modified pCIG plasmid with an additional human EIF4G

IRES (Wong et al., 2002) (Fig. 5A-C). We quantified five non-overlapping fields in the dorsolateral OE, dorsal to the transition zone where Sox2 levels rise, Ascl1 cells are seen, and Meis1 levels decline. This region contains neurons, as well as cells with more `medial' OE precursor characteristics (inset, Fig. 5A; see also Figs 1, 2). Ectopic elevation of Meis1, as well as Meis1/Pbx1, suppresses Ascl1 in dorsolateral OE cells (29±1.7% of 1632 control versus 15.4±1.7% of 718 Meis1 cells, P=0.001; 11.8±1.2% of 860 Meis1/Pbx1 cells, P<0.00005; Fig. 5D-I,N). There was no difference between Meis1 and Meis1/Pbx1, suggesting that Pbx co-factors are not required for this regulatory change. By contrast, elevated Meis1/Pbx1 levels do not suppress Sox2 (49.8±0.7%/903 control versus 49.2±1.5%/1125 Meis1/Pbx1 cells, P=0.7; Fig. 5J-M,O), suggesting Meis1-mediated Ascl1 suppression is independent of Sox2. We did not observe a change in TuJ1-labeled neurons (data not shown). This may reflect difficulties detecting changes among greater concentrations of already differentiated neurons in more dorsolateral OE regions, or the capacity of Meis1-expressing precursors that also express high levels of Sox to generate neurons – perhaps at a lower frequency independent of Ascl1 – as is seen in the ventromedial OE. Thus, a transcriptional network defined by Sox2 dose, Meis activity and antagonistic regulation of Ascl1 distinguishes primarily `lateral' from primarily `medial' OE precursors.

Ascl1 and Sox2 mutations yield predicted OE phenotypes

The transcriptional network defined by Sox2, Meis1 and Ascl1 provides a framework to confirm genetic relationships between OE precursor classes and OE neurogenesis. If Ascl1 is crucial for expanding but not specifying ORN, VRN and GnRH neuron populations, loss of Ascl1 function in *Ascl1*$^{-/-}$ mutant embryos should diminish but not prevent genesis of all three neuronal classes.

A high medial, low lateral Sox2 gradient and a substantial population of Meis1 cells are present in the *Ascl1*$^{-/-}$ OE (Fig. 6A,B). Meis1 cell frequency is somewhat higher in the mutant medial OE, and fewer laterally positioned Meis1 cells are acutely labeled with BrdU (Fig. 6C, compare with Fig. 2B), suggesting proliferative characteristics may be altered in precursors that have differing combinations of Sox2 as well as Meis1 expression levels in the absence of Ascl1 function. Only a small population of TuJ1-positive OE neurons remains in the E11.5 mutant (Fig. 6D; 29% of wild type values; $P \leq 0.02$, $n=4$, Mann-Whitney); nevertheless, ORNs, VRNs and GnRH neurons differentiate (Fig. 6E-L). OMP-labeled ORN frequency, however, is diminished by E16.5 (Fig. 6M). The small compliment of ORNs probably reflects limited early neurogenesis that declines to undetectable levels within 1 day of terminal division of an initial precursor cohort (Fig. 6I-N).

In our electroporation experiments, we found that elevated Sox2 suppresses Meis1 and promotes Ascl1 as well as neurogenesis (Fig. 4); therefore, it seemed that reduced Sox2 dose in vivo (*Sox2*$^{hyp/-}$) (Taranova et al., 2006) should expand Meis1, reduce or eliminate Ascl1, and diminish neurogenesis. Indeed, cells expressing Meis1/2 as well as Pbx genes are seen throughout the *Sox2*$^{hyp/-}$ OE (Fig. 7A-D; data not shown). Ascl1 cells are absent in the OE (Fig. 7E) but seen in the ventral forebrain (Fig. 7E, inset). S- and M-phase frequency declines in parallel with Meis1 precursor expansion (Fig. 7F-H). The number of TuJ1 neurons generated by E11.5 is significantly less than wild type (20%; $P \leq 0.02$, $n=4$, Mann-Whitney; Fig. 7I), similar to *Ascl1*$^{-/-}$ OE values. Reduced neuronal differentiation and failed VNO morphogenesis in *Sox2*$^{hyp/-}$ embryos parallels that in *Fgf8*$^{neo/neo}$ embryos (Fig. 3 and see Fig. S1D in the supplementary material), suggesting a relationship between Fgf8 signaling, Sox2 dose, VNO morphogenesis and OE neurogenesis. Nevertheless, all neuronal classes generated by the OE – ORNs, VRNs and

GnRH neurons – are seen in the *Sox2*$^{hyp/-}$ at E11.5 as well as at E6.5 (Fig. 7J-L). Thus, Sox2 dose is crucial for restricting Meis1 in the lateral OE, enhancing Ascl1 in the medial OE, and sustaining genesis – but not specification – of ORN, VRN and GnRH neurons.

DISCUSSION

We identified distinct precursor populations in the nascent OE that comprise self-renewing neural stem cells as well as transit amplifying cells that give rise to ORNs, VRNs and GnRH neurons. Meis1-expressing OE precursors, primarily in the lateral OE where neurons are absent or sparse, proliferate slowly and symmetrically to generate additional precursors. Proliferative cells that express high levels of Sox2, as well as Ascl1, primarily in the medial OE among differentiating neurons, divide rapidly and symmetrically to expand the OE neuronal population. Meis1, Sox2 and Ascl1 define a novel transcriptional network that regulates progression between these precursor states. Sox2 dose, controlled in part by local Fgf8 signaling, promotes OE neurogenesis by suppressing Meis1 and enhancing Ascl1 expression. Elevated Meis gene dose, independent of Pbx co-factors, diminishes Ascl1, but not Sox2 expression, and reduces neurogenesis by maintaining a more `lateral' precursor identity. This Fgf8-regulated, dose-dependent network balances self-renewal and terminal neurogenesis in the early embryonic OE.

Transcriptional profiles for OE precursors

Transcription factor profiles distinguish slowly dividing self-renewing from rapidly dividing transit amplifying OE precursors (Fig. 8A). As in other CNS regions, including the cerebral cortex (Bani-Yaghoub et al., 2006; Schuurmans and Guillemot, 2002), spinal cord (Graham et al., 2003) and retina (Heine et al., 2008; Taranova et al., 2006), OE precursors express SoxB1,

Meis and bHLH genes (Fig. 8A). Our analysis, although not exhaustive, illustrates that OE precursor classes are not identified by singular expression of any factor. Instead, relationships between graded expression – suggesting dose effects – define OE precursor identity. This expression-based identity of OE precursors corresponds approximately to `lateral' and `medial' OE regions; however, transcription factor gradients do not strictly respect these anatomical boundaries. Indeed, transition zones in the ventromedial as well as dorsolateral OE have cells with combinations of factors that may further distinguish proliferative capacity or fate; accordingly, there may be additional precursor classes than those defined here. Such observations may complicate planning or interpreting OE `transcriptional fate mapping' studies using recombination driven by single transcription factor loci: few OE precursors uniquely express any particular factor. Thus, alternative approaches may be needed to map OE lineages and fates, including local tracer injections combined with conditional recombination-based approaches.

Fgf8 and Sox2 act synergistically in the developing OE

The inductive signal Fgf8 and the transcription factor Sox2 regulate OE precursor identity and neurogenic capacity (Fig. 8B,C). Elevated Fgf8 levels alone are sufficient to elicit terminal symmetric neurogenic division from isolated `lateral' OE precursors – making them resemble `medial' OE precursors. When Fgf8 is reduced in the early OE by hypomorphic mutation, patterning is disrupted: Sox2 and Ascl1 levels decline, and Meis1 levels expand. Apparently, when Fgf8 is diminished, these cells acquire `lateral' precursor characteristics. The identity of `medial' OE precursors, and parallel morphogenesis of medial structures such as the VNO probably depend on maintaining high Sox2 levels, which in turn depend upon normal levels of

Fgf8. Accordingly, both *Fgf8* and *Sox2* hypomorphic OE phenotypes include Meis expansion, diminished Ascl1, failed VNO morphogenesis (without complete loss of the VRN marker TrpC2) and diminished neurogenesis (see also Kawauchi et al., 2005), without apparent loss of distinct OE neuron classes. Thus, precursors in *Fgf8* and *Sox2* hypomorphs – mostly expressing Meis1 – must include fate-specified multipotent OE neural stem cells.

A Sox2 dose-dependent transcriptional network defines OE precursors

We defined a transcriptional network that regulates progression of slowly dividing self-renewing to rapidly dividing terminal neurogenic OE precursors (Fig. 8B,C). Our results place Sox2 at a crucial, but distinct, position in specification of peripheral chemosensory versus other sensory receptor lineages, including hair cells (Dabdoub et al., 2008), taste cells (Okubo et al., 2006) and retinal precursors (Taranova et al., 2006). In contrast to Sox2 function in the ear, tongue and eye, where dose influences genesis of differentiated neuron subclasses, Sox2 in the nose is a concentration-dependent regulator of precursor state for the entire OE neuronal lineage. Direct electroporation in vitro as well as genetic manipulation in vivo indicates that low Sox2 dose maintains Meis1-expressing OE precursors. High Sox2 dose, modulated by Fgf8, facilitates the transition to terminally neurogenic precursors by inhibiting Meis1 and promoting Ascl1. Thus, Sox2 and Meis1 antagonistically (but not fully reciprocally; Fig. 8C) regulate Ascl1, which governs quantitative neurogenic output, but not identity, in the OE. As in the retina (Taranova et al., 2006), higher Sox2 dose might also modulate Notch and Hes expression or activity in the medial OE (Carson et al., 2006; Cau et al., 2000; Schwarting et al., 2007); however, it may be difficult to distinguish Sox2 and bHLH function in Notch-dependent mechanisms (Cau et al., 2000).

Sox2 dose is a crucial regulator of OE precursors via its influence on Meis genes. Elevated Sox2 in the lateral OE in vitro results in an effective local loss of Meis1 and Ascl1. We confirmed the relationship between Sox2 and Ascl1 in vivo using *Fgf8*$^{neo/neo}$ and *Asc1*$^{-/-}$ mutants; however, evaluating this relationship for Meis1, independent of Sox2 manipulation, remains challenging. We found no molecular, proliferative or neuronal defects in the OE of E11.5 *Meis1*$^{-/-}$ embryos (data not shown), perhaps because Meis1, Meis2 and Meis3, which are apparently redundant in other systems (Hisa et al., 2004), are co-expressed in the developing OE. Nevertheless, the effective gain of Meis1 function in the *Sox2*$^{hyp/-}$ OE reinforces the relationship between Sox2, Meis1 and Ascl1, and is consistent with dose-dependent influences of Sox2 on distinct OE precursor classes.

Meis1 OE precursors and OE neural stem cells

In the OE, Meis1 supports slowly dividing self-renewing precursors, whereas in retinal (Heine et al., 2008) and myogenic precursors (Berkes et al., 2004), it influences rapidly proliferating terminal-differentiating transit-amplifying precursors, perhaps via interactions with Pbx/Hox, bHLH genes and other factors. This suggests a novel function for Meis genes in the OE: suppression of bHLH genes to maintain slowly dividing self-renewing multipotent stem cells. Meis1-expressing OE precursors (Fig. 8B) conform to many criteria that define tissue-specific stem cells. They undergo slow symmetric self-renewing cell divisions (Gage, 2000; Slack, 2000), are found in a `niche' or distinct location (Fuchs et al., 2004; Moore and Lemischka, 2006), and generate all differentiated cell classes in a particular tissue. No other OE precursors have these characteristics, including capacity for `label retention' that distinguishes stem cells in other epithelia (Borthwick et al., 2001; Cotsarelis et al., 1990; Wong and Wright, 1999). Finally,

ORNs, VRNs and GnRH neurons are seen in *Ascl1*$^{-/-}$ and *Sox 2*$^{hyp/-}$ mutants, in parallel with expanded or potentially exclusive presence of Meis1-expressing precursors. This argues strongly that Meis1 OE precursor populations include fate-specified stem cells that yield all major types of OE neurons. We cannot, however, rule out additional heterogeneity among Meis1 precursors that leads to diversity of potential and fate as is the case for early retinal progenitors (for a review, see Marquardt and Gruss, 2002).

The lateral OE, perhaps owing to antagonism between lateral RA and medial Fgf8 signaling in the context of mesenchymal/epithelial (M/E) interaction (Bhasin et al., 2003; LaMantia et al., 2000), may provide a specific niche that maintains a substantial population of Meis1-expressing precursors. Only frontonasal M/E interactions establish this niche – probably owing to distinctive RA-producing neural crest that constitutes the lateral frontonasal mesenchyme (Anchan et al., 1997; LaMantia et al., 2000). Indeed, in vitro, excess RA diminishes Sox2 in the medial OE, whereas excess Fgf8 increases Sox2 in the lateral OE (Rawson et al., 2010). When Meis1 induction fails in the presumptive OE in vitro, due to altered M/E interactions (Rawson et al., 2010), neurons are generated, but ORNs, VRNs and GnRH neurons do not differentiate. The role of Meis1 OE precursors in generating non-neural supporting cells, which appear later in development (Asson-Batres and Smith, 2006), or ensheathing cells that migrate from the OE (Doucette, 1989) remains to be evaluated. Nevertheless, slowly dividing multipotent neural stem cells capable of generating ORNs, VRNs and GnRH neurons must be included among Meis1-expressing precursors found primarily in the lateral OE.

Defining OE neural stem cells throughout life

Our data provide new guidance for identifying adult OE neural stem cells, which have remained elusive despite their central importance in regeneration after OE injury (Nordin and Bramerson, 2008), and in psychiatric and neurodegenerative diseases (Feron et al., 1999; Hahn et al., 2005; Johnson et al., 1994). The distinct characteristics of embryonic OE precursors focus attention not only on molecular markers for adult counterparts, but on locations for a supportive niche, similar to those in other mature regenerating epithelia, including gut, lung and – in lower vertebrates – the retina (Borthwick et al., 2001; Hitchcock et al., 2004; Wong and Wright, 1999). If OE axes are systematically transformed between the embryo and the adult, neural stem cells should be sought along the lateral OE boundary with the respiratory epithelium. In this location, secreted factors (including RA) may maintain multipotent OE neural stem cells and antagonize signals involved in ORN maturation and zonal specification (Norlin et al., 2001). Indeed, cultures from human OE biopsies at this boundary generate cells with molecular and functional characteristics of ORNs (Borgmann-Winter et al., 2009). Thus, our results may facilitate study of nervous system regeneration, and provide insight into pathobiology of diseases that compromise olfaction as part of a broader spectrum of nervous system dysfunction.

Acknowledgments

In situ hybridization and confocal microscopy were performed in the UNC Neuroscience Center Expression Localization and Confocal Microscopy cores (National Institute of Neurological Diseases and Stroke, NS031768), with expert guidance from Y. Wu, M. Aita and R. Peterson. We are indebted to Thomas Sugimoto, Cliff Heindel and Amanda Peters, who provided excellent technical assistance in support of this work. National Institute of Child Health and Human

Development grant HD029178 (A.-S.L./N.R.) from the NIH and a Sigrid Jusélius Foundation Fellowship (M.K.L.) supported this work. Deposited in PMC for release after 12 months.

References

Ache B. W., Young J. M. *(2005). Olfaction: diverse species, conserved principles. Neuron 48, 417-430.*

Anchan R. M., Drake D. P., Haines C. F., Gerwe E. A., LaMantia A. S. *(1997). Disruption of local retinoid-mediated gene expression accompanies abnormal development in the mammalian olfactory pathway. J. Comp. Neurol. 379, 171-184.*

Asson-Batres M. A., Smith W. B. *(2006). Localization of retinaldehyde dehydrogenases and retinoid binding proteins to sustentacular cells, glia, Bowman's gland cells, and stroma: potential sites of retinoic acid synthesis in the postnatal rat olfactory organ. J. Comp. Neurol. 496, 149-171.*

Bani-Yaghoub M., Tremblay R. G., Lei J. X., Zhang D., Zurakowski B., Sandhu J. K., Smith B., Ribecco-Lutkiewicz M., Kennedy J., Walker P. R., et al. *(2006). Role of Sox2 in the development of the mouse neocortex. Dev. Biol. 295, 52-66.*

Beites C. L., Kawauchi S., Crocker C. E., Calof A. L. *(2005). Identification and molecular regulation of neural stem cells in the olfactory epithelium. Exp. Cell Res. 306, 309-316.*

Berkes C. A., Bergstrom D. A., Penn B. H., Seaver K. J., Knoepfler P. S., Tapscott S. J. *(2004). Pbx marks genes for activation by MyoD indicating a role for a homeodomain protein in establishing myogenic potential. Mol. Cell 14, 465-477.*

Bhasin N., Maynard T. M., Gallagher P. A., LaMantia A. S. *(2003). Mesenchymal/epithelial regulation of retinoic acid signaling in the olfactory placode. Dev. Biol. 261, 82-98.*

Borgmann-Winter K. E., Rawson N. E., Wang H. Y., Wang H., Macdonald M. L., Ozdener M. H., Yee K. K., Gomez G., Xu J., Bryant B., et al. *(2009). Human olfactory epithelial cells generated in vitro express diverse neuronal characteristics. Neuroscience 158, 642-653.*

Borthwick D. W., Shahbazian M., Krantz Q. T., Dorin J. R., Randell S. H. *(2001). Evidence for stem-cell niches in the tracheal epithelium. Am. J. Respir. Cell Mol. Biol. 24, 662-670.*

Buck L. B. *(2000). The molecular architecture of odor and pheromone sensing in mammals. Cell 100, 611-618.*

Carson C., Murdoch B., Roskams A. J. *(2006). Notch 2 and Notch 1/3 segregate to neuronal and glial lineages of the developing olfactory epithelium. Dev. Dyn. 235, 1678-1688.*

Cau E., Gradwohl G., Fode C., Guillemot F. *(1997). Mash1 activates a cascade of bHLH regulators in olfactory neuron progenitors. Development 124, 1611-1621.*

Cau E., Gradwohl G., Casarosa S., Kageyama R., Guillemot F. *(2000). Hes genes regulate sequential stages of neurogenesis in the olfactory epithelium. Development 127, 2323-2332.*

Cotsarelis G., Sun T. T., Lavker R. M. *(1990). Label-retaining cells reside in the bulge area of pilosebaceous unit: implications for follicular stem cells, hair cycle, and skin carcinogenesis. Cell 61, 1329-1337.*

Dabdoub A., Puligilla C., Jones J. M., Fritzsch B., Cheah K. S., Pevny L. H., Kelley M. W. *(2008). Sox2 signaling in prosensory domain specification and subsequent hair cell differentiation in the developing cochlea. Proc. Natl. Acad. Sci. USA 105, 18396-18401.*

DeHamer M. K., Guevara J. L., Hannon K., Olwin B. B., Calof A. L. *(1994). Genesis of olfactory receptor neurons in vitro: regulation of progenitor cell divisions by fibroblast growth factors. Neuron 13, 1083-1097.*

Donner A. L., Episkopou V., Maas R. L. *(2007). Sox2 and Pou2f1 interact to control lens and olfactory placode development. Dev. Biol. 303, 784-799.*

Doucette R. *(1989). Development of the nerve fiber layer in the olfactory bulb of mouse embryos. J. Comp. Neurol. 285, 514-527.*

Dulac C., Torello A. T. *(2003). Molecular detection of pheromone signals in mammals: from genes to behaviour. Nat. Rev. Neurosci. 4, 551-562.*

Ellis P., Fagan B. M., Magness S. T., Hutton S., Taranova O., Hayashi S., McMahon A., Rao M., Pevny L. *(2004). SOX2, a persistent marker for multipotential neural stem cells derived from embryonic stem cells, the embryo or the adult. Dev. Neurosci. 26, 148-165.*

Feron F., Perry C., Hirning M. H., McGrath J., Mackay-Sim A. *(1999). Altered adhesion, proliferation and death in neural cultures from adults with schizophrenia. Schizophr. Res. 40, 211-218.*

Foster D. L., Jackson L. M., Padmanabhan V. *(2006). Programming of GnRH feedback controls timing puberty and adult reproductive activity. Mol. Cell. Endocrinol. 254-255, 109-119.*

Fuchs E., Tumbar T., Guasch G. *(2004). Socializing with the neighbors: stem cells and their niche. Cell 116, 769-778.*

Gage F. H. *(2000). Mammalian neural stem cells. Science 287, 1433-1438.*

Garel S., Huffman K. J., Rubenstein J. L. *(2003). Molecular regionalization of the neocortex is disrupted in Fgf8 hypomorphic mutants. Development 130, 1903-1914.*

Gotz M., Huttner W. B. *(2005). The cell biology of neurogenesis. Nat. Rev. Mol. Cell Biol. 6, 777-788.*

Graham V., Khudyakov J., Ellis P., Pevny L. *(2003). SOX2 functions to maintain neural progenitor identity. Neuron 39, 749-765.*

Guillemot F., Lo L. C., Johnson J. E., Auerbach A., Anderson D. J., Joyner A. L. *(1993). Mammalian achaete-scute homolog 1 is required for the early development of olfactory and autonomic neurons. Cell 75, 463-476.*

Hahn C. G., Gomez G., Restrepo D., Friedman E., Josiassen R., Pribitkin E. A., Lowry L. D., Gallop R. J., Rawson N. E. *(2005). Aberrant intracellular calcium signaling in olfactory neurons from patients with bipolar disorder. Am. J. Psychiatry 162, 616-618.*

Heine P., Dohle E., Bumsted-O'Brien K., Engelkamp D., Schulte D. *(2008). Evidence for an evolutionary conserved role of homothorax/Meis1/2 during vertebrate retina development. Development 135, 805-811.*

Hisa T., Spence S. E., Rachel R. A., Fujita M., Nakamura T., Ward J. M., Devor-Henneman D. E., Saiki Y., Kutsuna H., Tessarollo L., et al. *(2004). Hematopoietic, angiogenic and eye defects in Meis1 mutant animals. EMBO J. 23, 450-459.*

Hitchcock P., Ochocinska M., Sieh A., Otteson D. *(2004). Persistent and injury-induced neurogenesis in the vertebrate retina. Prog. Retin. Eye Res. 23, 183-194.*

Jessell T. M., Sanes J. R. *(2000). Development. The decade of the developing brain. Curr. Opin. Neurobiol. 10, 599-611.*

Johnson G. S., Basaric-Keys J., Ghanbari H. A., Lebovics R. S., Lesch K. P., Merril C. R., Sunderland T., Wolozin B. *(1994). Protein alterations in olfactory neuroblasts from Alzheimer donors. Neurobiol. Aging 15, 675-680.*

Kawauchi S., Shou J., Santos R., Hebert J. M., McConnell S. K., Mason I., Calof A. L. *(2005). Fgf8 expression defines a morphogenetic center required for olfactory neurogenesis and nasal cavity development in the mouse. Development 132, 5211-5223.*

LaMantia A. S., Bhasin N., Rhodes K., Heemskerk J. *(2000). Mesenchymal/epithelial induction mediates olfactory pathway formation. Neuron 28, 411-425.*

Livesey F. J., Cepko C. L. *(2001). Vertebrate neural cell-fate determination: lessons from the retina. Nat. Rev. Neurosci. 2, 109-118.*

Marquardt T., Gruss P. *(2002). Generating neuronal diversity in the retina: one for nearly all. Trends Neurosci. 25, 32-38.*

Martynoga B., Morrison H., Price D. J., Mason J. O. *(2005). Foxg1 is required for specification of ventral telencephalon and region-specific regulation of dorsal telencephalic precursor proliferation and apoptosis. Dev. Biol. 283, 113-127.*

Meyers E. N., Lewandoski M., Martin G. R. *(1998). An Fgf8 mutant allelic series generated by Cre- and Flp-mediated recombination. Nat. Genet. 18, 136-141.*

Moore K. A., Lemischka I. R. *(2006). Stem cells and their niches. Science 311, 1880-1885.*

Morshead C. M., Reynolds B. A., Craig C. G., McBurney M. W., Staines W. A., Morassutti D., Weiss S., van der Kooy D. *(1994). Neural stem cells in the adult mammalian forebrain: a relatively quiescent subpopulation of subependymal cells. Neuron 13, 1071-1082.*

Nordin S., Bramerson A. *(2008). Complaints of olfactory disorders: epidemiology, assessment and clinical implications. Curr. Opin. Allergy Clin. Immunol. 8, 10-15.*

Norlin E. M., Alenius M., Gussing F., Hagglund M., Vedin V., Bohm S. *(2001). Evidence for gradients of gene expression correlating with zonal topography of the olfactory sensory map. Mol. Cell. Neurosci. 18, 283-295.*

Okubo T., Pevny L. H., Hogan B. L. *(2006). Sox2 is required for development of taste bud sensory cells. Genes Dev. 20, 2654-2659.*

Rawson N. E., Lischka F., Yee K. K., Peters A. Z., Tucker E. S., Meechan D. W., Zirlinger M., Maynard T. M., Burd G. B., Dulac C., et al. *(2010). Specific mesenchymal/epithelial induction of olfactory receptor, vomeronasal, and gonadotropin-releasing hormone (GnRH) neurons. Dev. Dyn. 239, 1723-1738.*

Schuurmans C., Guillemot F. *(2002). Molecular mechanisms underlying cell fate specification in the developing telencephalon. Curr. Opin. Neurobiol. 12, 26-34.*

Schwanzel-Fukuda M., Pfaff D. W. *(1989). Origin of luteinizing hormone-releasing hormone neurons. Nature 338, 161-164.*

Schwarting G. A., Gridley T., Henion T. R. *(2007). Notch1 expression and ligand interactions in progenitor cells of the mouse olfactory epithelium. J. Mol. Histol. 38, 543-553.*

Schwob J. E. *(2002). Neural regeneration and the peripheral olfactory system. Anat. Rec. 269, 33-49.*

Shen Q., Zhong W., Jan Y. N., Temple S. *(2002). Asymmetric Numb distribution is critical for asymmetric cell division of mouse cerebral cortical stem cells and neuroblasts. Development 129, 4843-4853.*

Slack J. M. *(2000). Stem cells in epithelial tissues. Science 287, 1431-1433.*

Stowers L., Holy T. E., Meister M., Dulac C., Koentges G. *(2002). Loss of sex discrimination and male-male aggression in mice deficient for TRP2. Science 295, 1493-1500.*

Taranova O. V., Magness S. T., Fagan B. M., Wu Y., Surzenko N., Hutton S. R., Pevny L. H. *(2006). SOX2 is a dose-dependent regulator of retinal neural progenitor competence. Genes Dev. 20, 1187-1202.*

Toresson H., Parmar M., Campbell K. *(2000). Expression of Meis and Pbx genes and their protein products in the developing telencephalon: implications for regional differentiation. Mech. Dev. 94, 183-187.*

Tucker E. S., Polleux F., LaMantia A. S. *(2006). Position and time specify the migration of a pioneering population of olfactory bulb interneurons. Dev. Biol. 297, 387-401.*

Wong E. T., Ngoi S. M., Lee C. G. *(2002). Improved co-expression of multiple genes in vectors containing internal ribosome entry sites (IRESes) from human genes. Gene Ther. 9, 337-344.*

Wong W. M., Wright N. A. *(1999). Cell proliferation in gastrointestinal mucosa. J. Clin. Pathol. 52, 321-333.*

Wray S., Grant P., Gainer H. *(1989). Evidence that cells expressing luteinizing hormone-releasing hormone mRNA in the mouse are derived from progenitor cells in the olfactory placode. Proc. Natl. Acad. Sci. USA 86, 8132-8136.*

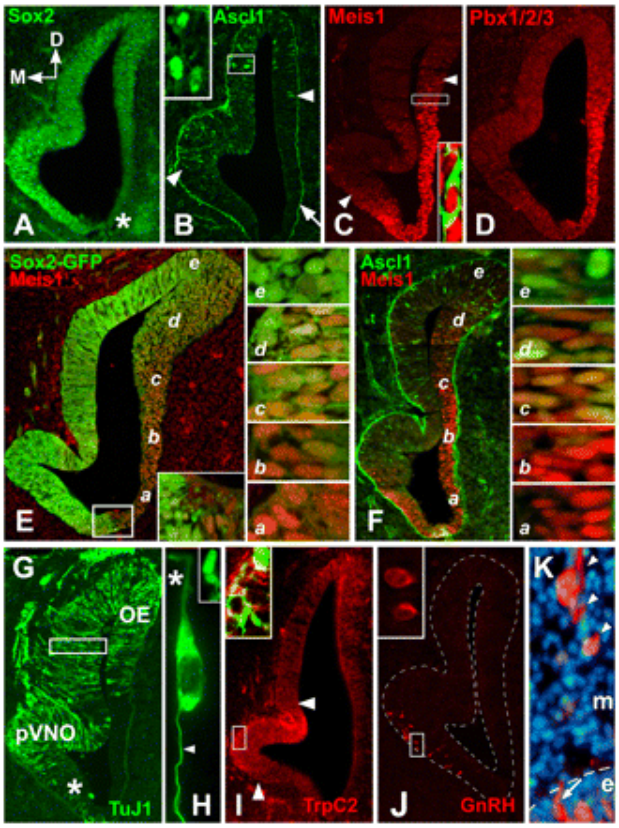

Fig. 1.

Molecularly distinct domains in the E11.5 mouse OE. (**A**) Graded Sox2 expression is highest in the medial presumptive vomeronasal organ (pVNO), and lowest ventrolaterally (asterisk). (**B**) Ascl1 is expressed from the dorsolateral OE through medial pVNO region (between arrowheads), mostly overlapping high Sox2 expression; arrow indicates non-specific basal lamina labeling. Inset: higher magnification of the boxed region shows Ascl1-positive nuclei. (**C**) Meis1 expression begins ventromedially, peaks in the lateral OE and declines dorsolaterally. Inset: higher magnification of region boxed shows nuclear Meis1 in nascent TuJ1-labeled OE neurons. (**D**) Pbx1/2/3 is expressed in the lateral OE and, like Meis1 expression, declines dorsally. (**E**) Graded expression of Sox2 (Sox2-eGFP reporter) and Meis1 is complementary. There is a sharp ventral boundary (box, inset). *a-e* indicate the levels of sections shown in the panels on the right. Varying levels of complementary Sox2 and Meis1 expression are found in cells at distinct ventrolateral (*a*) to dorsomedial (*e*) locations. Little if any Meis1 is seen dorsally (*e*) where Sox2 predominates. (**F**) Ascl1 and Meis1 are also complementary; however, robust Ascl1 labeling begins only in dorsomedial locations (*d, e*, right panels), where Meis1 is nearly undetectable. (**G**) TuJ1-labeled OE neurons are seen at low frequency dorsolaterally, become concentrated dorsomedially through the pVNO and decline to a few scattered cells in the extreme ventromedial OE (asterisk). Box indicates region shown in H. (**H**) TuJ1-labeled OE neurons have cytological hallmarks of ORNs and VRNs: a single apical process (asterisk), apparent `dendritic knob' (inset) and a single axon (arrowhead). (**I**) VRNs are distinguished by enhanced expression of TrpC2 (red) within the pVNO (between arrowheads), apparently on the cell surface of TuJ1-labeled neurons (green, inset). (**J**) GnRH neurons are seen within, or ventral to, the pVNO. Inset: higher magnification of boxed region, showing two GnRH neurons within the ventromedial OE. (**K**) GnRH neurons delaminate from the OE (arrow, e) and migrate through the frontonasal mesenchyme (arrowheads, m).

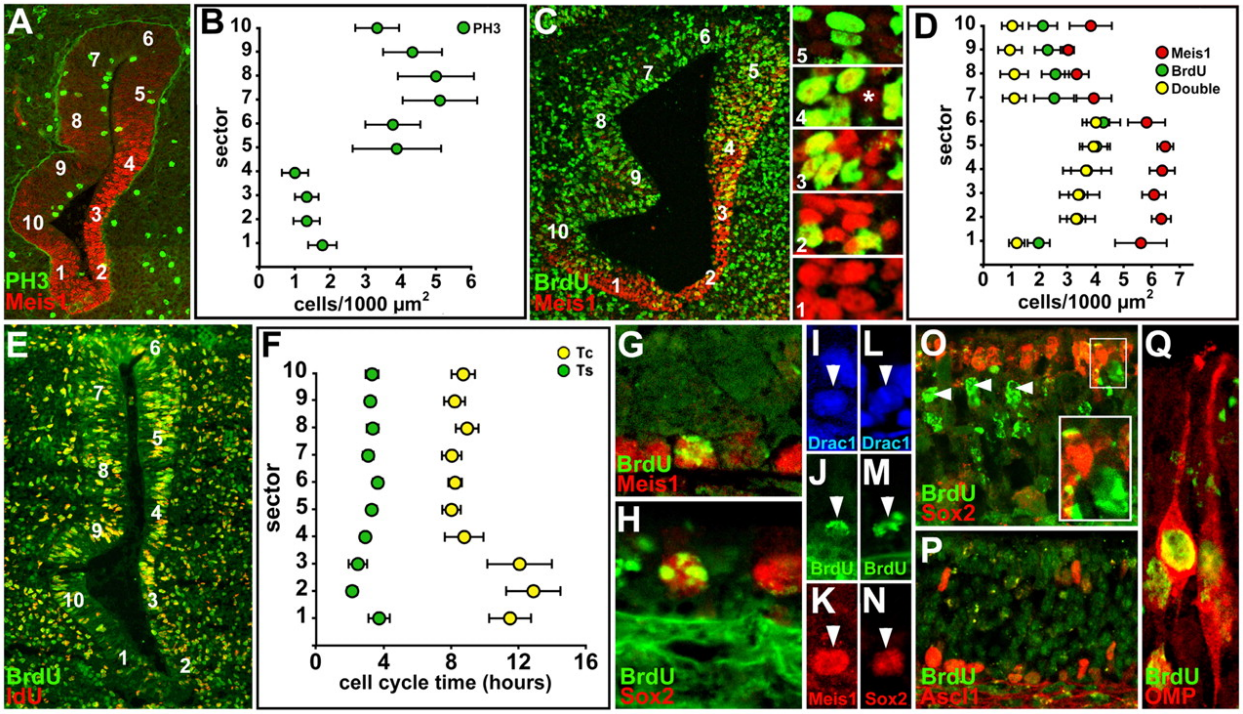

Fig. 2.

OE precursors have distinct proliferative characteristics. (**A**) PH3 labeled cells (M-phase) are less frequent in lateral versus medial OE. (**B**) Counts of PH3 cells in 10 geometrically defined OE s ectors (positions are indicated in A) confirm enhanced M-phase cell frequency in dorsomedial versus ventrolateral regions. (**C**) Acute BrdU labeling increases ventro- to dorsolaterally, and declines in register with diminishing levels of Meis1. (Insets) There are scattered cells lightly labeled with Meis1 (e.g. asterisk in sector 4 image) in medial regions (sectors 6-10). (**D**) Counts of BrdU, Meis1 and double-labeled cells in 10 equivalent OE sectors (positions are indicated in A) confirm inverse Meis1 and S-phase frequency. We counted lightly Meis1 labeled cells (* in panel 4), yielding a lower frequency of Meis1 cells especially in sectors 7-10. (**E**) Cell cycle times estimated using dual S-phase labeling. IdU/BrdU-labeled cells (yellow), BrdU-alone (green) and all cells (bisbenzimide; not shown) are counted to calculate cell cycle time (Tc) and S-phase duration (Ts). (**F**) Tc and Ts in OE sectors 1-10 (positions are indicated in E). (**G**) Precursors that retain BrdU for long periods (5 days, `label-retaining') are found in lateral E16.5 OE and express Meis1. (**H**) Similar label-retaining lateral precursors express Sox2. (**I-K**) A single cell in separate color channels shows nuclear, BrdU, and Meis1 labeling. (**L-N**) A similar color separation of a label-retaining cell confirms nuclear Sox2 expression. (**O**) Heavily BrdU-labeled medial cells (arrowheads) do not coincide with high Sox2 cells in medial E16.5 OE. Inset: higher magnification of boxed area shows an example of a lightly BrdU-labeled high Sox2-expressing medial OE cell. (**P**) Label-retaining medial cells rarely if ever coincide with Ascl1 in the medial E16.5 OE. (**Q**) Many heavily BrdU-labeled medial cells at E16.5 are ORNs, based upon dual labeling with the ORN marker OMP.

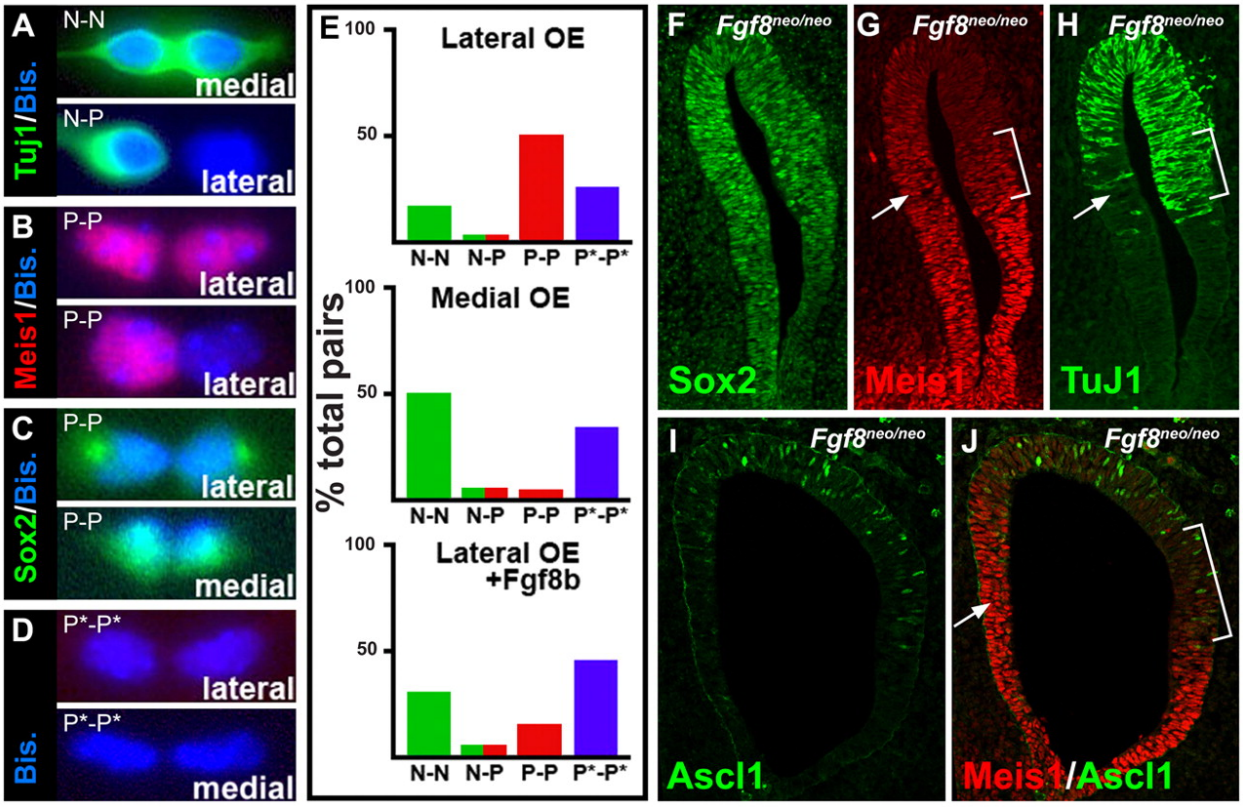

Fig. 3.

OE precursors have distinct modes of division and Fgf8-dependent neurogenic potential. (**A-D**) Examples of neuron (TuJ1 N, nuclear counterstain with bis-benzamide), precursor (Meis1 or Sox2, P) or nuclear (bisbenzamide only, P^* pairs cultured from microdissected lateral and medial E11.5 OE. (**E**) Histograms show frequency of N-N (green, TuJ1 labeled), N-P (green-red, TuJ1 and Sox2 or Meis1), P-P (red, Meis1 or Sox2 labeled) or P^*-P^*(bis-benzamide only) pairs from lateral (top) and medial OE cells (middle). Bottom histogram shows influence of exogenous Fgf8 added to the culture medium on frequency of pairs generated by lateral OE cells. (**F-J**) In vivo consequences of reduced Fgf8 levels shown for two Fgf8 hypomorphic mouse embryos. (F) Sox2 levels are diminished in the medial OE, and a distinct mediolateral gradient is difficult to discern. (G) Meis1 expression diminishes in the dorsolateral OE (bracket), but expands into the medial OE (arrow). (H) TuJ1-positive neurons are reduced medially (arrow) and shifted laterally (bracket). (I) Ascl1-positive precursors diminish in the medial OE and shift laterally, matching TuJ1 distribution in the hypomorphic OE. (J) Meis1 and Ascl1 double-labeling shows medial loss of Ascl1 and coincident expansion of Meis1 (arrow), as well as Ascl1 lateral expansion where Meis1 declines (bracket).

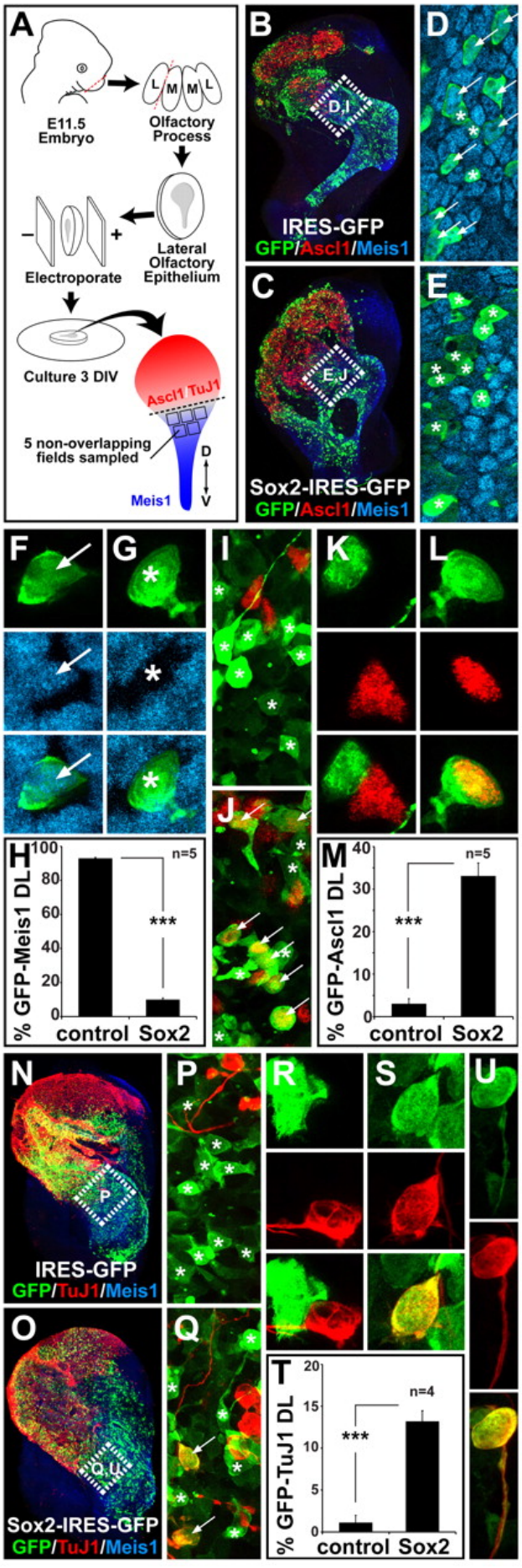

Fig. 4.

Sox2 dose regulates OE precursor identity. (**A**) Schematic of E11.5 lateral OE explant electroporation, culture and sampling strategy. Confocal images show (**B**) control eGFP or (**C**) pCIG-Sox2-electroporated lateral OE. Boxed areas in all panels indicate regions examined for illustration and quantification. Lower (**D**,**E**) and higher (**F**,**G**) magnification confocal images show Meis1 co-expression (cyan, arrows) or lack thereof (asterisks) in control (D,F) or Sox2-electroporated (E,G) GFP-positive (green) OE cells. (**H**) Effects of elevated Sox2 dose on Meis1 cell frequency. Lower (**I**,**J**) and higher (**K**,**L**) magnification images show lack of Ascl1 expression (asterisks) in control cells (I,K) and enhanced Ascl1 expression (red, arrows) in Sox2-electroporated (J,L) cells. (**M**) Effects of elevated Sox2 dose on Ascl1 cell frequency. Confocal images show TuJ1-labeled neurons in control (**N**) and Sox2-electroporated (**O**) lateral OE. Lower (**P**,**Q**) and higher (**R**,**S**) magnification images show lack of coincidence (asterisks) with TuJ1 neurons (red) in control (P,R) or an increase (arrows) in Sox2-electroporated (Q,S) cells. (**T**) Effects of elevated Sox2 dose on TuJ1-labeled neuron frequency. (**U**) Higher magnification images show a Sox2-electroporated TuJ1-labeled neuron with a single apparent axon. $^{*}P \leq 0.0002$.

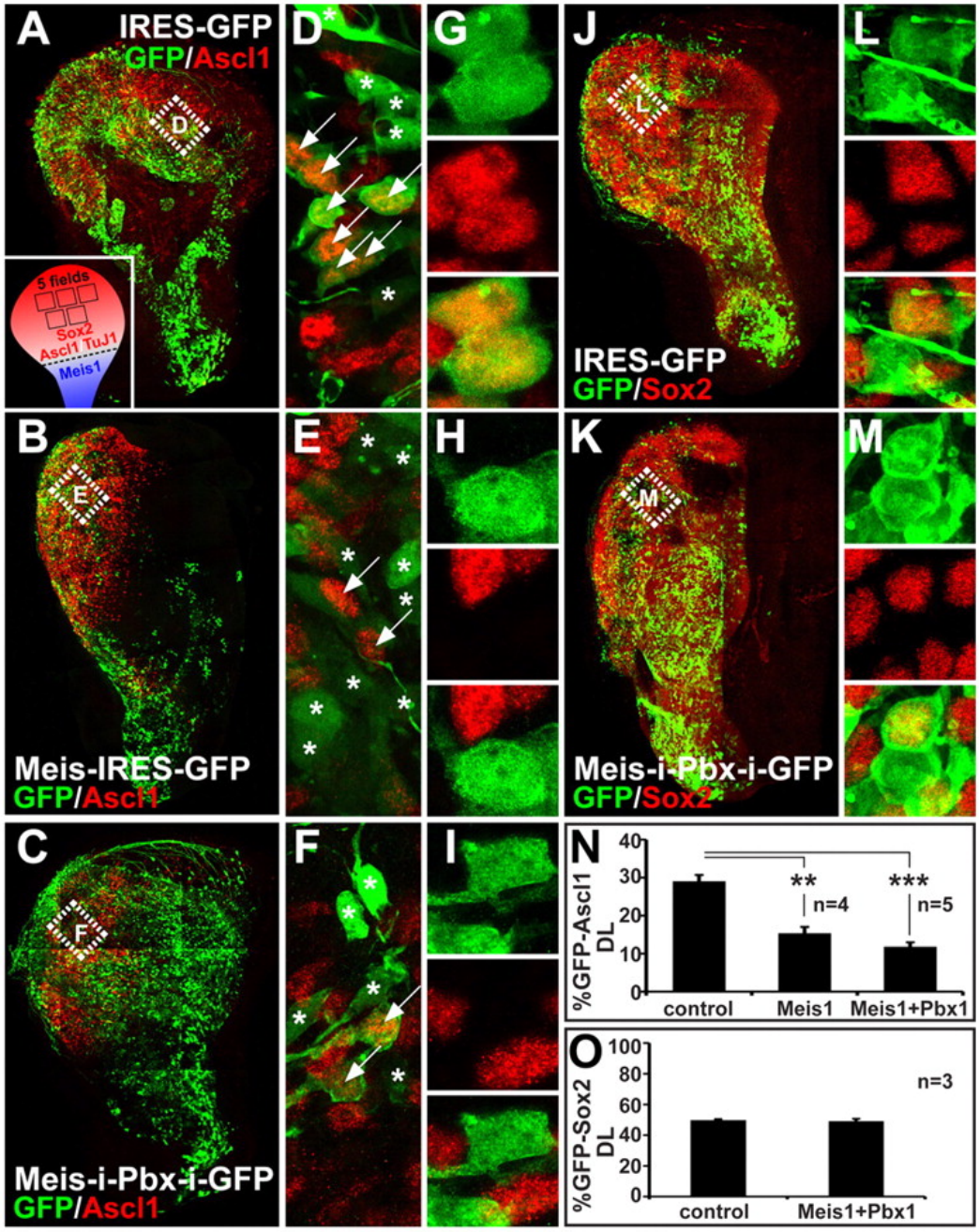

Fig. 5.

Meis1 regulates OE precursor identity. (**A-C**) Confocal images show E11.5 lateral OE preparations electroporated with control (A), pCIG-Meis1 (B) or pCIG-Meis1-IRES-Pbx1 (C) and labeled for Ascl1. Inset in A shows area illustrated and sampled for Meis1 overexpression experiments. Boxed areas represent regions used for illustration and quantification. Lower (**D-F**) and higher (**G-I**) magnification comparison of Ascl1 expression in control (D,G), Meis1 (E,H) or Meis1/Pbx1 (F,I) electroporated cells in the dorsolateral OE. (**J**,**K**) Images showing E11.5 control (J) and Meis1/Pbx1 (K) electroporated preparations labeled for Sox2. (**L**,**M**) Sox2 is seen in control (L) and Meis1/Pbx1 (M) electroporated cells in the dorsolateral OE. (**N**) Frequency of GFP-Ascl1 doubled-labeled cells in control, Meis1 and Meis1/Pbx1 electroporated preparations. (**O**) Frequency of GFP-Sox2 double-labeled cells in control and Meis1-Pbx1 electroporated preparations. $^{**}P \leq 0.002$; $^{***}P \leq 0.0002$.

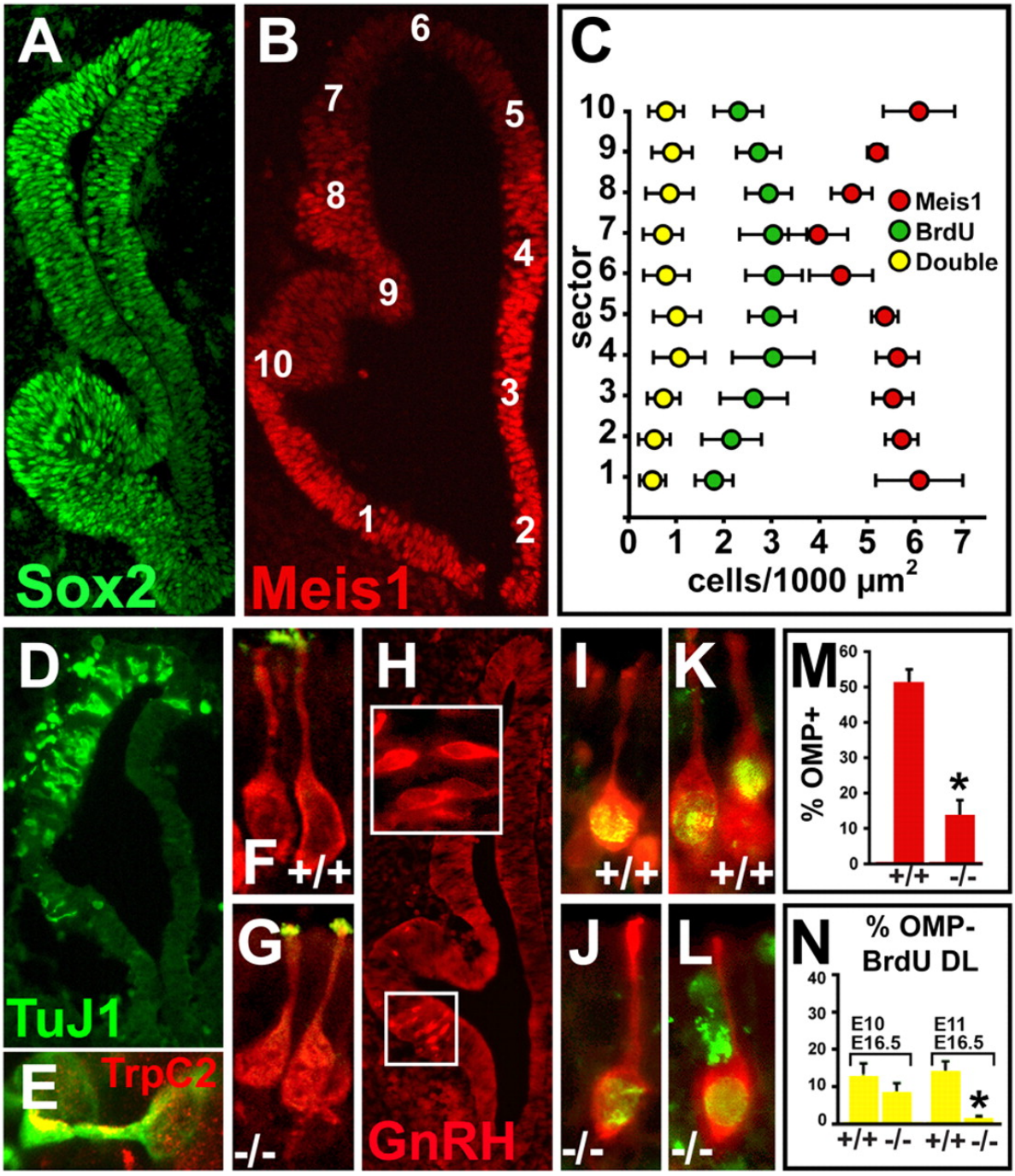

Fig. 6.

Precursor and neuron identity in the *Ascl1*$^{-/-}$ mutant OE. (**A**) The Sox2 medial-lateral gradient is preserved in the E11.5 OE. (**B**) Heavily labeled Meis1 cells remain concentrated in the lateral OE in *Ascl1*$^{-/-}$ E11.5 mouse embryos, whereas moderately labeled cells expand medially. (**C**) Frequency and distribution of Meis1 cells, acutely labeled BrdU cells and Meis1/BrdU double-labeled cells is altered in the *Ascl1*$^{-/-}$ OE. Positions of the cells are indicated in B. (**D**) Limited neuronal differentiation, recognized with TuJ1, is seen in the E11.5 *Ascl1*$^{-/-}$ OE. (**E**) TrpC2 (red) expression can still be detected in a small subset of *Ascl1*$^{-/-}$ OE neurons (green). (**F**,**G**) OMP and the ORN-selective adenylyl cyclase ACIII (green) are expressed and localized appropriately in *Ascl1*$^{-/-}$ ORNs at E16.5. (**H**) GnRH neurons are generated in or near the pVNO in *Ascl1*$^{-/-}$ embryos. (**I-L**) ORNs in the E16.5 *Ascl1*$^{-/-}$ OE are birthdated with BrdU at E10 (earliest ORN genesis; I, J) and E11 (K,L). (**M**) Frequency of OMP-positive ORNs in the E16.5 *Ascl1*$^{-/-}$ OE is substantially reduced. (**N**) Near-normal frequency of ORN genesis at E10 declines to near zero by E11 in the E16.5 *Ascl1*$^{-/-}$ OE. $^{*}P \leq 0.02$.

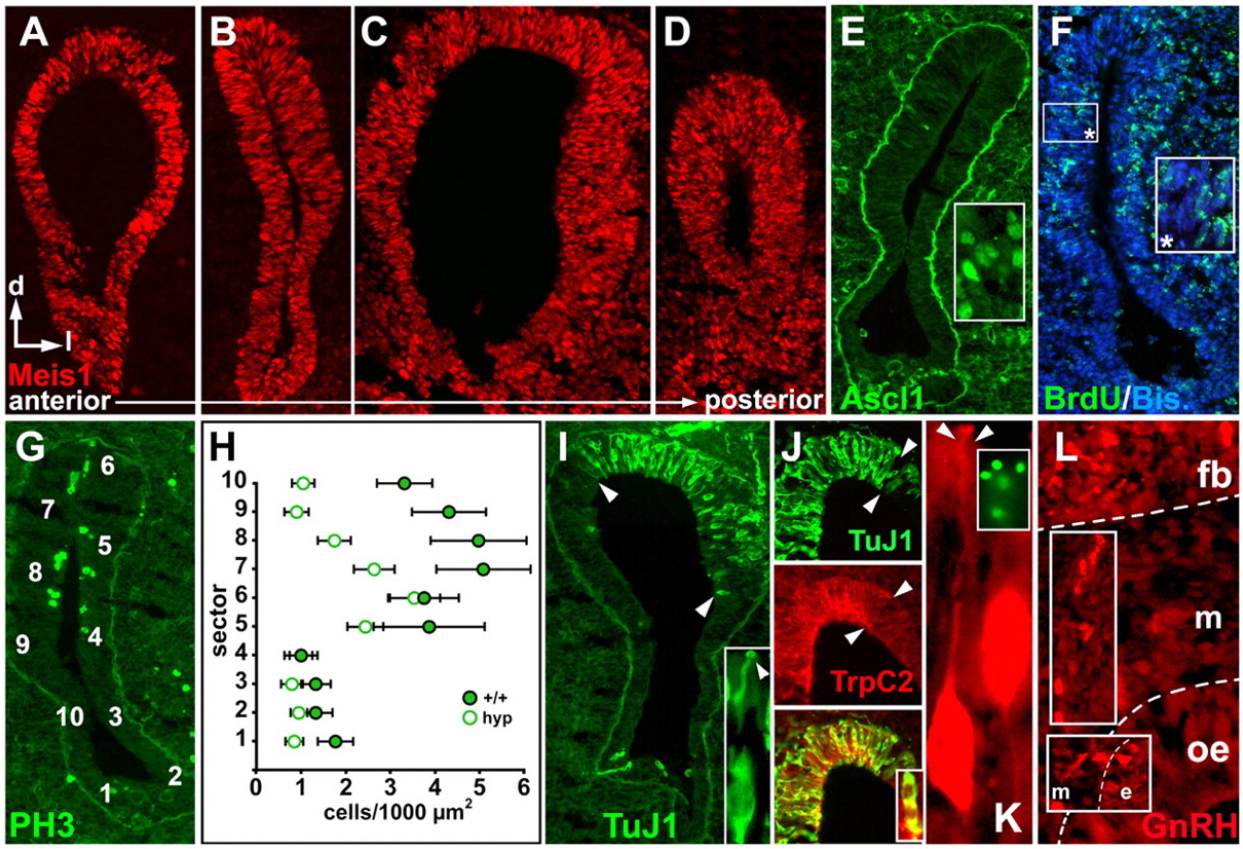

Fig. 7.

Precursor and neuron identity in the *Sox2*$^{hyp/-}$ OE. (**A-D**) Meis1 cells are distributed throughout the OE over the entire anteroposterior axis in *Sox2*$^{hyp/-}$ mouse embryos. (**E**) Ascl1 is not detected in *Sox2*$^{hyp/-}$ OE, but is seen in MGE precursors in the forebrain (Inset). (**F**) Acute BrdU labeling is substantially diminished in *Sox2*$^{hyp/-}$ OE. Scattered BrdU-positive cells are nevertheless detectable (inset). (**G**,**H**) Frequency of PH3-labeled mitotic cells diminishes towards lateral values in dorsomedial sectors of the *Sox2*$^{hyp/-}$ OE. The positions of the cells are indicated in G. (**I**) Neuronal differentiation is attenuated in the *Sox2*$^{hyp/-}$ OE. TuJ1-labeled neurons are seen dorsally (arrowheads) and their frequency is diminished (compare with Fig. 1G). (**J**) TrpC2 remains expressed in the E11.5 *Sox2*$^{hyp/-}$ OE. Arrowheads indicate the dorsomedial OE where both TuJ1- and TrpC2-labeled neurons are seen in the *Sox2*$^{hyp/-}$.(**K**) A small number of ORNs that express OMP (red) and ACIII (green, inset) differentiate by E16.5 in the *Sox2*$^{hyp/-}$ OE. Arrowheads indicate the dendritic knob of an OMP-labeled ORN in the *Sox2*$^{hyp/-}$ OE. Inset is at higher magnification showing that ACIII is localized to this dendritic knob, as in wild-type E16.5 ORNS (see Fig.6F). (**L**) GnRH neurons are still detected, although at lower frequencies, in the *Sox2*$^{hyp/-}$ OE, adjacent mesenchyme (m) and ventral forebrain (fb). The lower inset shows GnRH-labeled cells in the OE (e), as well as the adjacent mesenchyme (m) of the E11.5 *Sox2*$^{hyp/-}$. The upper inset shows several GnRH-labeled cells in the frontonasal mesenchyme (m).

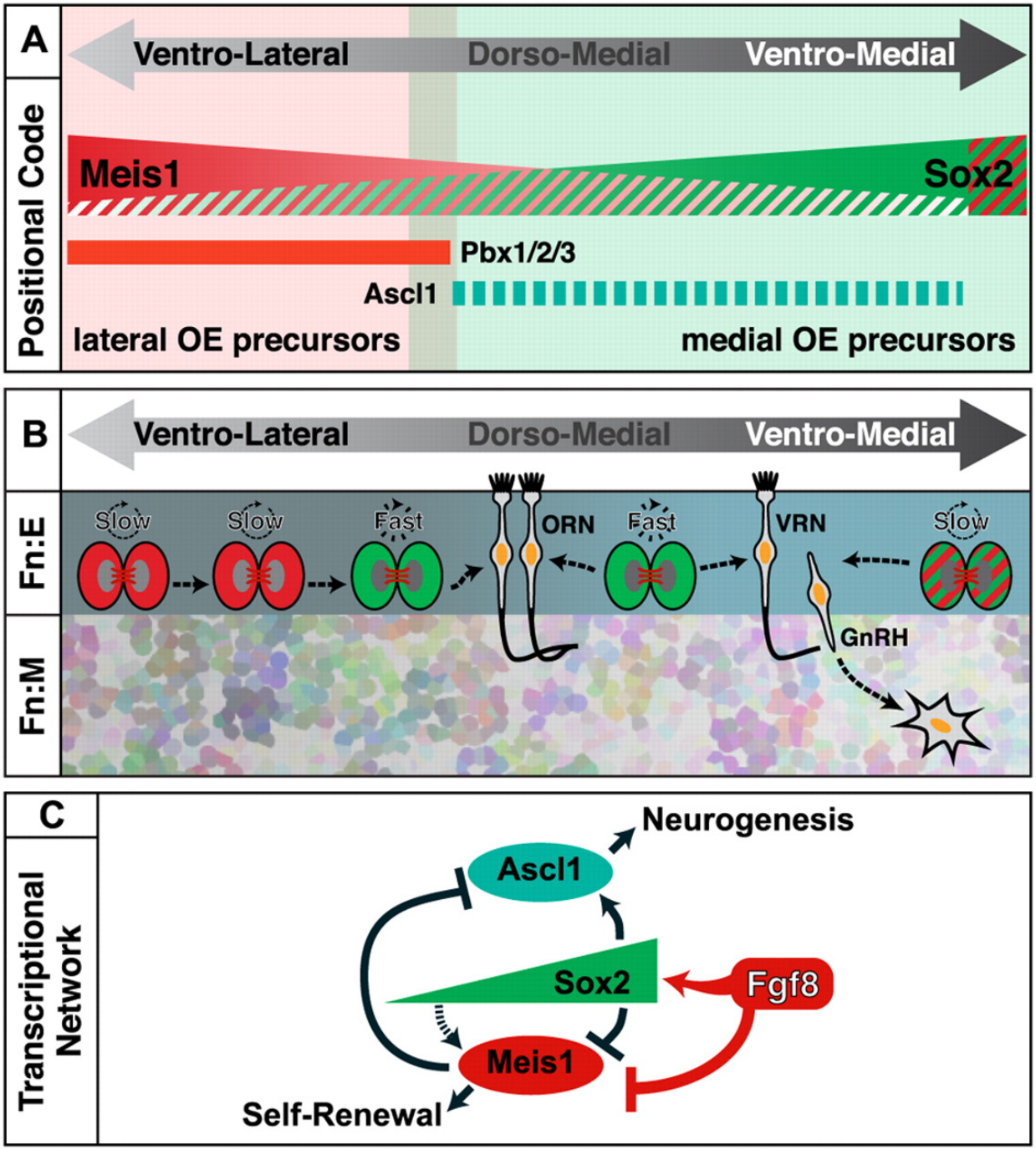

Fig. 8.

Distinct molecular and cellular identities of OE precursors. (**A**) Precursor identity is established by OE position and reflected in combinatorial graded transcription factor expression. (**B**) Meis1 defines slowly dividing self-renewing precursors, primarily in the lateral OE; enhanced Sox2, coincident with Ascl1 and increased Fgf8 signaling, identifies transit amplifying precursors, primarily in the medial OE, that are responsible for quantitative expansion, but not specification of ORNs, VRNs and GnRH neurons. Slowly dividing precursors in the ventro-medial OE express both Meis1 and Sox2 at high levels (A), and may contribute to genesis of GnRH cells and/or VRNs, which populate this region. (**C**) A Sox2 dose-dependent transcriptional network, modulated by Fgf8, preserves lateral slowly dividing, multipotent OE precursors by maintaining low Sox2 levels that support Meis1 expression, or promotes medial transit amplifying cells that expand OE neuron numbers by Fgf8-dependent high Sox2-mediated downregulation of Meis1 and parallel upregulation of Ascl1.

Fig. S1. Mediolateral patterning defects in the hypomorphic Fgf8 olfactory epithelium. (**A**) Frontonasal process of wild-type Fgf8 littermate stained with TuJ1 (green), Meis1 (red), and bisbenzimide (blue). (**B**) Higher magnification of box in A showing normal lateral restriction of Meis1 domain, and prominent neuronal differentiation in the medial OE. (**C-L**) Three independent *Fgf8*$^{neo/neo}$ mutant embryos show similar patterning deficits, failed pVNO morphogenesis and abnormal forebrain development, including rostromedial protrusion of ventral telencephalic tissue (arrows). (C) Frontonasal process of an *Fgf8* hypomorph stained as in A. (D) Higher magnification of box in C showing medial expansion of Meis1 (arrowhead) and accompanying loss of TuJ1-positive neurons in the medial OE. (E) Frontonasal process of second *Fgf8* hypomorph stained with Ascl1 (green), Meis1 (red) and bisbenzimide (blue). (F) Higher magnification of box in E showing medial expansion of Meis1 (arrowhead) and reduction in Ascl1 labeling in the medial OE. (G,H). Third Fgf8 hypomorph at two positions (2, 5) along the anteroposterior axis recapitulated in I-L. (I) Meis1 expression is shifted medially (arrowheads), particularly at rostral levels, of the nascent OE. (J) TuJ1 staining is reduced in the medial OE in register with medial expansion of Meis1. (K) Sox2 levels are reduced medially, leveling its medial-high/lateral-low graded expression pattern throughout the entire AP axis of the OE. (L) Ascl1 expression is reduced and fewer brightly labeled nuclei are present in the medial OE.